Synthesis of Carbaborane Rhodium–Platinum Complexes: Crystal Structure of $[RhPt(\mu\text{-}H)(\mu\text{-}CO)(PEt_3)_2(PPh_3)(\eta^5\text{-}7,9\text{-}C_2B_9H_{11})]$ *

Justin E. Goldberg, Donald F. Mullica, Eric L. Sappenfield and F. Gordon A. Stone
Department of Chemistry, Baylor University, Waco, TX 76798-7348, USA

Treatment of $[PtCl(H)(PEt_3)_2]$ with $[NEt_4][Rh(CO)(PPh_3)(\eta^5\text{-}7,9\text{-}C_2B_9H_{11})]$ in thf (tetrahydrofuran) in the presence of $TlBF_4$ affords $[RhPt(\mu\text{-}H)(\mu\text{-}CO)(PEt_3)_2(PPh_3)(\eta^5\text{-}7,9\text{-}C_2B_9H_{11})]$, the structure of which has been established by X-ray diffraction. On heating at reflux in thf for several days the compound yields $[RhPt(\mu\text{-}\sigma\text{:}\eta^5\text{-}7,9\text{-}C_2B_9H_{10})(CO)(PEt_3)_2(PPh_3)]$, a product in which the rhodium–platinum bond is spanned by an exopolyhedral cage B–Pt linkage. Reactions between the platinum compounds $[PtCl(R)L_2]$ (R = Me or Ph; L = PEt_3, PPh_3 or PMe_2Ph) and $[NEt_4][Rh(CO)(PPh_3)(\eta^5\text{-}7,n\text{-}C_2B_9H_{11})]$ (n = 8 or 9) afford several dimetal complexes in which the Rh–Pt bonds are bridged by exopolyhedral cage B–H ⟶ Pt or B–Pt bridge bonds. The latter are formed from the former by loss of RH molecules, and this process is favoured for $Rh(\eta^5\text{-}7,9\text{-}C_2B_9H_{11})$ *versus* $Rh(\eta^5\text{-}7,8\text{-}C_2B_9H_{11})$, and in the order L = PPh_3 < PMe_2Ph < PEt_3 for the ligands on platinum. The NMR data (^1H, $^{13}C\text{-}\{^1H\}$, $^{11}B\text{-}\{^1H\}$ and $^{31}P\text{-}\{^1H\}$) are reported and discussed in relation to the structures of the products.

We have shown that the salts $[NEt_4][Rh(CO)L(\eta^5\text{-}7,8\text{-}C_2B_9H_9R_2)]$ (L = CO or PPh_3, R = H or Me) can be used to prepare mixed-metal compounds with bonds between rhodium and cobalt,[1a] iridium,[1a] platinum,[1b] rhenium,[1c] copper[1d] and gold.[1d,e] These syntheses followed recognition that the anionic rhodium complexes are isolobal with $[Fe(CO)_2(\eta\text{-}C_5H_5)]^-$, and that salts of the latter species have been successfully employed in the preparation of mixed-metal complexes for many years.[2] An important feature of these reactions of the carbaboranerhodium salts is that in the products the cage ligand frequently adopts a non-spectator role, bridging the metal–metal linkages *via* exopolyhedral B–H ⟶ M (M = Co or Au) or B–M (Ir or Re) bonds. It seems probable that the species with B–M bonds form from intermediates with B–H ⟶ M linkages. Moreover, involvement of the cage in exopolyhedral bonding is more favoured if the rhodium salt employed in the syntheses contains an $\eta^5\text{-}C_2B_9H_9Me_2$ group rather than the $\eta^5\text{-}C_2B_9H_{11}$ ligand. The methyl groups in the former serve to activate preferentially the BH vertex in the open pentagonal C_2B_3 face ligating the metal which is β to the two carbons.

The compounds containing B–M linkages form with the C_2B_9 cages an unusual cluster system. Similar attachment of the carbaborane framework to a dimetal unit has been identified in other species, including the tungsten–platinum compounds $[WPt(\mu\text{-}H)\{\mu\text{-}\sigma\text{:}\eta^5\text{-}7,8\text{-}C_2B_9H_7(CH_2C_6H_4Me\text{-}4)\text{-}10\text{-}Me_2\text{-}7,8\}(CO)_2(PMe_3)(PEt_3)_2]$ **1**[3a] and $[WPt(\mu\text{-}CC_6H_3Me_2\text{-}2,6)(\mu\text{-}\sigma\text{:}\eta^5\text{-}7,8\text{-}C_2B_9H_8Me_2)(CO)_3(PEt_3)]$ **2**,[3b] derived from reactions between the anionic alkylidynetungsten complexes $[W(\equiv CR)(CO)_2(\eta^5\text{-}7,8\text{-}C_2B_9H_9Me_2)]^-$ (R = C_6H_4Me-4 or $C_6H_3Me_2$-2,6) and platinum salts.

In this paper we describe several reactions of the salts $[NEt_4][Rh(CO)(PPh_3)(\eta^5\text{-}7,8\text{-}C_2B_9H_{11})]$ **3a** and $[NEt_4][Rh(CO)(PPh_3)(\eta^5\text{-}7,9\text{-}C_2B_9H_{11})]$ **3b** which afford products in which the carbaborane cage bridges a Rh–Pt bond *via* B–H ⟶ Pt or B–Pt linkages. No reactions of **3b** with platinum compounds have been reported previously, but the complex $[RhPt(\mu\text{-}H)(\mu\text{-}CO)(PEt_3)_2(PPh_3)(\eta^5\text{-}7,8\text{-}C_2B_9H_{11})]$ **4a** has been prepared by treating **3a** with $[PtCl(H)(PEt_3)_2]$ in acetone in the presence of $TlBF_4$.[1b] However, in **4a** the carbaborane ligand adopts a spectator role.

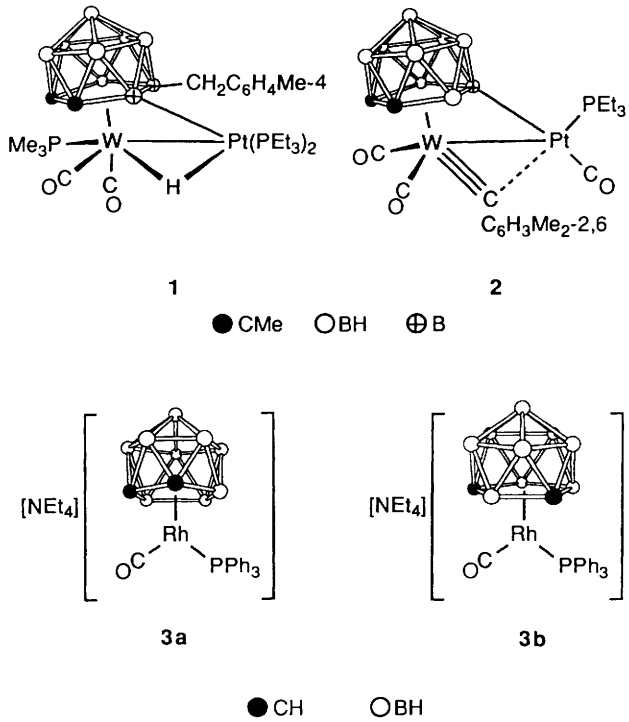

Results and Discussion

In thf (tetrahydrofuran), in the presence of $TlBF_4$, equimolar amounts of compounds **3b** and *trans*-$[PtCl(H)(PEt_3)_2]$ afford $[RhPt(\mu\text{-}H)(\mu\text{-}CO)(PEt_3)_2(PPh_3)(\eta^5\text{-}7,9\text{-}C_2B_9H_{11})]$ **4b**, a product similar to the species **4a**. Some data characterising complex **4b** are given in Table 1, and an X-ray diffraction study

* *Supplementary data available:* see Instructions for Authors, *J. Chem. Soc., Dalton Trans.*, 1992, Issue 1, pp. xx–xxv.

was carried out, as had been done earlier with **4a**.[1b] The relevant data for **4b** are given in Table 2, and the structure of the molecule is shown in Fig. 1.

As expected, many of the structural parameters for compound **4b** are similar to those for **4a**. Thus the Rh–Pt bond distances are 2.734(2) and 2.748(1) Å, respectively. Other comparable data (**4a**, **4b**) are: μ-C(O)–Rh 1.99(1), 1.978(7); μ-C(O)–Pt 1.99(1), 2.014(8) Å; Rh–μ-C–O 133(1), 132.3(6); Pt–μ-C–O 141(1), 140.7(6)°; P–Pt_{av} 2.305(4), 2.308(2); Rh–P 2.257(4), 2.312(2) Å. The atom H(1) was not detected in the Fourier difference map of **4b** and it was therefore fixed: Pt–H(1) 1.757, Rh–H(1) 1.477 Å. The μ-H ligand was located in the X-ray diffraction study of **4a** and its position refined [Pt–H 1.8(2), Rh–H 1.7(2) Å].

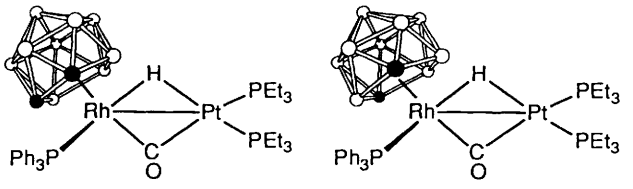

4a **4b**

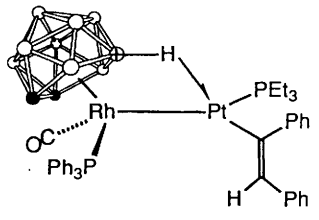

5

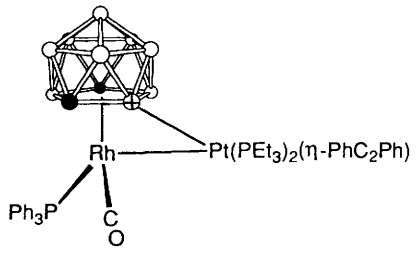

6

● CH ○ BH ⊕ B

The B–B bond distances associated with the upper pentagonal plane and apical cap of the *nido*-icosahedral 7,9-$C_2B_9H_{11}$ cage of compound **4b** are uniform [mean B–B 1.76(2), range 1.72–1.79 Å]. However, a distortion is observed between the two antiprism pentagonal planes in the $C_2B_9H_{11}$ cage. This is evidenced by the inequality in metrics between the B–B and C–B connectivities connecting the two planes [mean B–B 1.82(1), mean C–B 1.71(1); ranges 1.80–1.84 and 1.69–1.73 Å, respectively]. Further, a slight distortion is also observed when examining the lower open-faced pentagonal plane of the cage, *i.e.* atoms C(1), C(2), B(4) and B(5) are planar to within 0.005 Å, whereas atom B(3) is located 0.240 Å from the mean plane. Nevertheless, when considering the five atoms of the plane in relationship to the ring B(6)–B(10), parallelism exists (dihedral angle of 0.49°). The distance between the rhodium atom and the centroid of the open face of the *nido*-$C_2B_9H_{11}$ is 1.735 Å. The average bond angle within both pentagonal rings is 108°.

The C_2B_3 open face in structure **4a**[1b] is planar, whereas in structure **4b** it is somewhat distorted, with a slightly folded ring [see atom B(3) in Fig. 1]. Similar features have been encountered by Hawthorne and co-workers[4] in studies on other carbaboranerhodium species with [*nido*-7,*n*-$C_2B_9H_{11}$]$^{2-}$ (*n* = 8 or 9) groups. The conclusions to be drawn from their studies and those in this paper are that polyhedral distortions occur more severely for rhodacarbaboranes derived from the [*nido*-7,9-$C_2B_9H_{11}$]$^{2-}$ ligand than for those derived from [*nido*-7,8-$C_2B_9H_{11}$]$^{2-}$. Examination of the data in Table 2 for the Rh–C(1,2) and Rh–B(3,4,5) connectivities, and those of B(3)–C(1,2), C(1)–B(5), C(2)–B(4) and B(4)–B(5), shows the

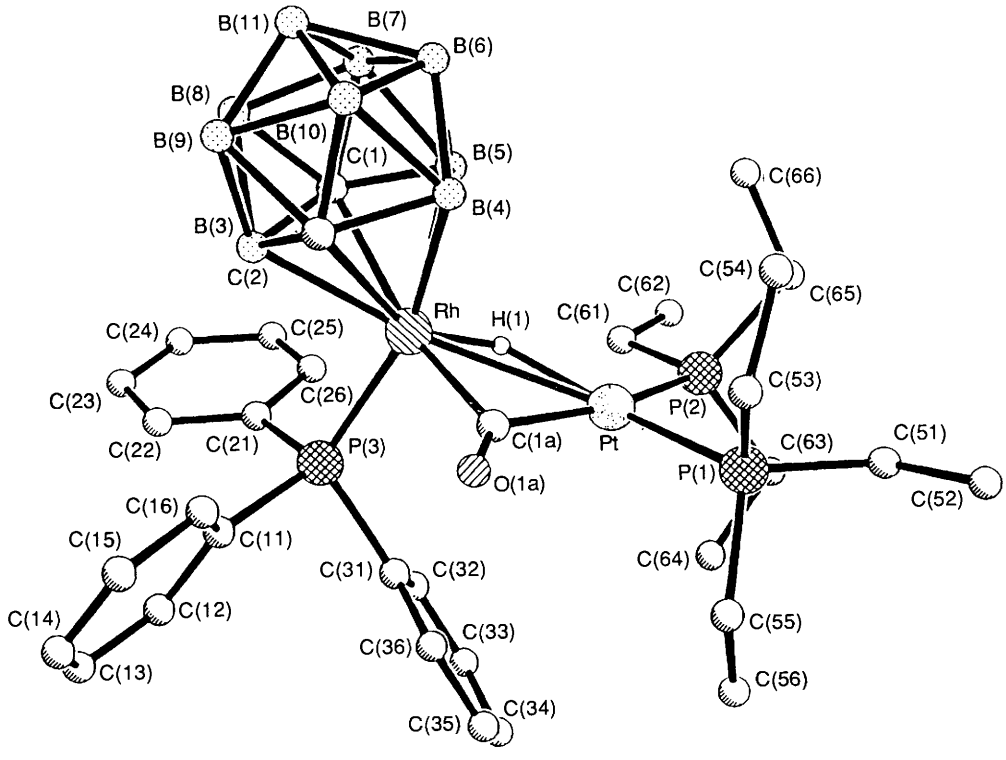

Fig. 1 Molecular structure of the complex [RhPt(μ-H)(μ-CO)$(PEt_3)_2(PPh_3)$(η^5-7,9-$C_2B_9H_{11}$)] **4b**, showing the atom labelling scheme

Table 1 Analytical[a] and physical data for the rhodium–platinum complexes

Compound	Colour	Yield (%)	$\tilde{\nu}_{max}$(CO)[b]/cm^{-1}	Analysis (%) C	H
4b [RhPt(μ-H)(μ-CO)(PEt_3)$_2$(PPh_3)(η^5-7,9-$C_2B_9H_{11}$)]	Orange	83	1766s	40.5 (41.4)	5.8 (6.0)
6 [RhPt(μ-σ:η^5-7,9-$C_2B_9H_{10}$)(CO)(PEt_3)$_2$(PPh_3)(η-PhC_2Ph)]	Yellow	92	1954vs	49.4 (49.8)	6.0 (5.8)
7a [RhPt(μ-σ:η^5-7,9-$C_2B_9H_{10}$)(CO)(PEt_3)$_2$(PPh_3)]	Yellow	91	1958vs	41.6 (41.5)	5.8 (5.8)
7b [RhPt(μ-σ:η^5-7,9-$C_2B_9H_{10}$)(CO)$_2$(PPh_3)$_2$]	Ochre	45	2046vs, 1993m	47.2 (47.6)	3.6 (4.0)
7c [RhPt(μ-σ:η^5-7,9-$C_2B_9H_{10}$)(CO)(PMe_2Ph)$_2$(PPh_3)]	Mustard yellow	73	1954vs	44.7 (44.7)	5.0 (4.7)
8c [RhPtPh(CO)(PPh_3)$_2$(η^5-7,9-$C_2B_9H_{11}$)][c]	Mustard yellow		1996vs		
8d [RhPtMe(CO)(PMe_2Ph)(PPh_3)(η^5-7,9-$C_2B_9H_{11}$)][c]	Yellow		1990vs		
9a [RhPt(μ-σ:η^5-7,8-$C_2B_9H_{10}$)(CO)(PEt_3)$_2$(PPh_3)]	Yellow-green	35	1975vs	42.1 (41.5)	6.1 (5.8)
9b [RhPt(μ-σ:η^5-7,8-$C_2B_9H_{10}$)(CO)(PMe_2Ph)$_2$(PPh_3)]	Green	37	1980vs	43.9 (44.7)	5.3 (4.7)
10b [RhPtPh(CO)(PPh_3)$_2$(η^5-7,8-$C_2B_9H_{11}$)]	Yellow-green	61	2005vs	50.6 (51.0)	4.5 (4.4)
10c [RhPtMe(CO)(PMe_2Ph)(PPh_3)(η^5-7,8-$C_2B_9H_{11}$)][c]	Yellow	39[d]	1996vs		

[a] Calculated values are given in parentheses. [b] Measured in CH_2Cl_2. All spectra show a broad band at *ca.* 2550 cm^{-1} due to B–H absorptions. [c] Microanalytical data not available because compound decomposes to form a complex with a B–Pt bond, see text. [d] Crude yield, see Experimental section.

Table 2 Selected internuclear distances (Å) and angles (°) for the complex [RhPt(μ-H)(μ-CO)(PEt_3)$_2$(PPh_3)(η^5-7,9-$C_2B_9H_{11}$)] **4b**

Pt–Rh	2.748(1)	Pt–P(1)	2.282(2)	Pt–P(2)	2.334(2)	Pt–H(1)*	1.757
Pt–C(1a)	2.014(8)	Rh–P(3)	2.312(2)	Rh–H(1)*	1.477	Rh–C(1a)	1.978(7)
Rh–C(1)	2.352(8)	Rh–B(3)	2.217(9)	Rh–C(2)	2.310(7)	Rh–B(4)	2.251(9)
Rh–B(5)	2.252(9)	C(1a)–O(1a)	1.192(9)	C(1)–B(3)	1.732(12)	C(1)–B(5)	1.685(12)
C(1)–B(7)	1.713(13)	C(1)–B(8)	1.686(12)	B(3)–C(2)	1.741(11)	B(3)–B(8)	1.837(14)
B(3)–B(9)	1.830(13)	C(2)–B(4)	1.685(12)	C(2)–B(9)	1.732(12)	C(2)–B(10)	1.704(12)
B(4)–B(5)	1.838(13)	B(4)–B(6)	1.796(14)	B(4)–B(10)	1.818(14)	B(5)–B(6)	1.812(13)
B(5)–B(7)	1.825(13)	B(6)–B(7)	1.778(13)	B(6)–B(10)	1.754(14)	B(6)–B(11)	1.763(15)
B(7)–B(8)	1.749(15)	B(7)–B(11)	1.754(14)	B(8)–B(9)	1.761(14)	B(8)–B(11)	1.789(14)
B(9)–B(10)	1.758(14)	B(9)–B(11)	1.765(15)	B(10)–B(11)	1.718(14)	P(1)–C(51)	1.828(9)
P(1)–C(53)	1.818(9)	P(1)–C(55)	1.840(10)	P(2)–C(61)	1.814(8)	P(2)–C(63)	1.820(10)
P(2)–C(65)	1.819(9)	P(3)–C(11)	1.838(8)	P(3)–C(21)	1.843(8)	P(3)–C(31)	1.853(9)
Rh–Pt–P(1)	135.3(1)	Rh–Pt–P(2)	119.9(1)	P(1)–Pt–P(2)	102.6(1)	P(1)–Pt–H(1)	162.5(1)
P(2)–Pt–H(1)	91.2(1)	Rh–Pt–C(1a)	46.0(2)	P(1)–Pt–C(1a)	92.0(2)	P(2)–Pt–C(1a)	165.3(2)
Pt–Rh–P(3)	100.9(1)	P(3)–Rh–H(1)	95.0(1)	Pt–Rh–C(1a)	47.0(2)	P(3)–Rh–C(1a)	93.7(2)
Pt–H(1)–Rh	116.1(1)	Pt–C(1a)–Rh	87.0(3)	Pt–C(1a)–O(1a)	140.7(6)	Rh–C(1a)–O(1a)	132.3(6)

	Distance (Ph)		Angle (Ph)	
Ring	Mean	Range	Mean	Range
C(11)–C(16)	1.38(2)	1.34–1.40	120.0(7)	118.8–120.8
C(21)–C(26)	1.38(1)	1.36–1.40	120.0(12)	117.9–121.8
C(31)–C(36)	1.37(1)	1.35–1.39	120.0(10)	118.6–121.5

* Fixed distance (see text).

distortion in metrics of the *nido*-icosahedral 7,9-$C_2B_9H_{11}$ cage in **4b**. The severity of distortion of the ligating cage fragment is not, however, as pronounced in our results as that observed earlier.[4]

The spectroscopic data for compound **4b** are in agreement with the structure established by X-ray diffraction. In the IR spectrum the band for the μ-CO group occurs at 1766 cm^{-1}, to be compared with that observed in the spectrum of **4a** at 1764 cm^{-1}. In the ^{1}H NMR spectrum (Table 3) the signal for the μ-H ligand is at δ −6.76, appearing as a doublet [*J*(PH) 70 Hz] with ^{195}Pt satellite peaks [*J*(PtH) 396 Hz]. The resonance was too broad to observe coupling with two of the phosphorus nuclei and with the rhodium, unlike the spectrum of **4a** where the corresponding signal (δ −5.85) is split by the three non-equivalent ^{31}P nuclei and the ^{103}Rh nucleus [*J*(PH) 79, 20, 20, *J*(RhH) 12, *J*(PtH) 431 Hz].[1b] In the ^{13}C-{^{1}H} NMR spectrum (Table 3) diagnostic signals for the cage CH groups were seen at δ 46.2 and 47.2, but no CO resonance was observed, a feature we attribute to a weak spectrum and the fact that the signal would be split by coupling with ^{103}Rh and the non-equivalent ^{31}P nuclei. The ^{31}P-{^{1}H} NMR spectrum of **4b** (Table 4) showed the expected three resonances and these were seen at δ 4.2 [PPt, *J*(PtP) 2699], 21.1 [PPt, *J*(RhP) 13, *J*(PtP) 4131] and 36.7 [PRh, *J*(RhP) 126 Hz]. The ^{31}P NMR data for **4a** are very similar.

Compound **4a** in thf reacts slowly (*ca.* 3 d) with PhC≡CPh to give [RhPt{σ-C(Ph)=C(Ph)H}(CO)(PEt_3)(PPh_3)(η^5-7,8-$C_2B_9H_{11}$)] **5**.[1b] In contrast, compound **4b** under similar conditions does not react with the alkyne. However, when heated to reflux in the presence of PhC≡CPh it affords [RhPt(μ-σ:η^5-7,9-$C_2B_9H_{10}$)(CO)(PEt_3)$_2$(PPh_3)(η-PhC_2Ph)] **6**, in which the alkyne is η^2-co-ordinated to the platinum. The presence of the exopolyhedral B–Pt bond in **6** is clearly revealed by the ^{11}B-{^{1}H} NMR spectrum (Table 4). A deshielded resonance is seen at δ 42.9 with strong ^{195}Pt–^{11}B coupling (659 Hz). The other ^{11}B signals are observed as broad peaks in the range δ 1.3 to −26.9, as is typical for BH vertices. The peak for the B–Pt linkage may be compared with the corresponding resonances seen in the ^{11}B-{^{1}H} NMR spectra of **1** and **2** at δ 36.2 [*J*(PtB) 400] and 47.0 [*J*(PtB) 508 Hz], respectively.[3] The ^{31}P-{^{1}H} NMR spectrum (Table 4) is as expected, showing three resonances in a 1:1:1 ratio; one ^{31}P nucleus on rhodium [δ 35.8, *J*(RhP) 149 Hz], and two on platinum [δ 26.2, *J*(PtP) 1910; and δ 13.5, *J*(PtP) 4875 Hz]. The difference in the value of

Table 3 Hydrogen-1 and carbon-13 NMR data[a] for the complexes

Compound	^1H[b] (δ)	^{13}C[c] (δ)
4b	−6.76 [d, br, 1 H, μ-H, *J*(PH) 70, *J*(PtH) 396], 0.93 (m, 9 H, CH_2Me), 1.06 (m, 9 H, CH_2Me), 1.87 (m, 6 H, CH_2Me), 1.98 (m, 7 H, CH_2Me and CH of $C_2B_9H_{11}$), 2.16 (s, 1 H, CH of $C_2B_9H_{11}$), 7.28–7.51 (m, 15 H, Ph)	135.7 [d, C^1 (Ph), *J*(PC) 41], 134.1 [d, C^2 (Ph), *J*(PC) 11], 130.2 [d, C^4 (Ph), *J*(PC) 2], 128.4 [d, C^3 (Ph), *J*(PC) 10], 47.2, 46.2 ($C_2B_9H_{11}$), 20.9 [d, CH_2, *J*(PC) 27, *J*(PtC) 31], 16.7 [d of d, CH_2, *J*(PC) 31 and 2, *J*(PtC) 46], 8.8 [Me, *J*(PtC) 20], 8.4 [d, Me, *J*(PC) 2, *J*(PtC) 28]
6	0.67 [d of t, 9 H, CH_2Me, *J*(PH) 15, *J*(HH) 8], 1.13 [d of t, 9 H, CH_2Me, *J*(PH) 17, *J*(HH) 8], 1.57 (m, 6 H, CH_2Me), 2.12 (m, 7 H, CH_2Me and CH of $C_2B_9H_{10}$), 2.29 (s, 1 H, CH of $C_2B_9H_{10}$), 6.64–7.68 (m, 25 H, Ph)	196.4 [d of d, CO, *J*(RhC) 74, *J*(PC) 17], 145.0–125.0 (Ph and C≡C), 52.2, 43.5 ($C_2B_9H_{10}$), 19.6 [d of d, CH_2, *J*(PC) 34 and 5, *J*(PtC) 42], 18.6 [d, CH_2, *J*(PC) 20, *J*(PtC) 17], 9.1 [d, Me, *J*(PC) 2, *J*(PtC) 32], 8.5 [Me, *J*(PtC) 11]
7a	0.94 (m, br, 18 H, CH_2Me), 1.34, 1.69, 1.93 (m, br × 3, 13 H, CH_2Me and CH of $C_2B_9H_{10}$), 2.60 (s, 1 H, CH of $C_2B_9H_{10}$), 7.33–7.59 (m, 15 H, Ph)	195.2 [d of d of t, CO, *J*(RhC) 73, *J*(PC) 18 and 7], 135.2, 134.3, 130.2, 128.6 (Ph),[d] 53.0, 42.8 ($C_2B_9H_{10}$), 19.4 [CH_2, *J*(PtC) 38], 19.1 [CH_2, *J*(PtC) 35], 9.0, 8.9 (Me)
7b	0.59, 2.61 (s × 2, 2 H, CH of $C_2B_9H_{10}$), 7.38–7.65 (m, 30 H, Ph)	192.3 [d of d, CO, *J*(RhC) 74, *J*(PC) 18], 134.3–128.6 (Ph), 52.1, 43.2 ($C_2B_9H_{10}$)
7c[e]	0.98, *1.04 (s, br, 1 H, CH of $C_2B_9H_{10}$), 1.07, *1.08, *1.12, 1.22 [d × 2, 6 H, Me, *J*(PH) 7], 1.46, *1.53, 1.74, *1.76 [d × 2, 6 H, Me, *J*(PH) 11], 2.63, *2.82 (s, br, 1 H, CH of $C_2B_9H_{10}$), 7.04–7.70 (m, 25 H, Ph)	194.8 [d of d, CO, *J*(RhC) 72, *J*(PC) 16], *194.6 [d of d, CO, *J*(RhC) 75, *J*(PC) 19], 141.0–125.9 (Ph), *51.3, 45.3 ($C_2B_9H_{10}$), 19.6–17.7 (m, Me)
8c[f]	−5.30 [q, 1 H, BHPt, *J*(BH) 82, *J*(PtH) 361], 1.94, 2.40 (s × 2, 2 H, CH of $C_2B_9H_{11}$), 6.34–7.70 (m, 35 H, Ph)	
8d[e,f]	−4.07 [q, br, 1 H, BHPt, *J*(BH) 85], *−3.08 [q, br, 1 H, BHPt, *J*(BH) 79],[g] 0.49 [d, 3 H, MePt, *J*(PH) 4, *J*(PtH) 86], *0.54, 0.67 (s, br, 1 H, CH of $C_2B_9H_{11}$), 0.85 (m, 6 H, MeP), *1.13, *1.31 (m × 2, 6 H, MeP), 2.79, *2.96 (s, 1 H, CH of $C_2B_9H_{11}$), 7.21–7.88 (m, 20 H, Ph)	
9a	0.85 [d of t, 9 H, CH_2Me, *J*(PH) 15, *J*(HH) 7], 1.05 [d of t, 9 H, CH_2Me, *J*(PH) 16, *J*(HH) 8], 1.65 (m, 4 H, CH_2Me), 1.76 (s, br, 2 H, CH of $C_2B_9H_{10}$), 1.93, 1.99 (m × 2, 8 H, CH_2Me), 7.37–7.67 (m, 15 H, Ph)	196.8 [d of d, CO, *J*(RhC) 77, *J*(PC) 19], 134.3, 134.1, 130.6, 128.9 (Ph),[d] 44.4, 40.7 ($C_2B_9H_{10}$), 20.3 [CH_2, *J*(PtC) 30], 20.1 [CH_2, *J*(PtC) 42], 9.2, 8.9 (Me)
9b	1.03, 1.16 [d × 2, 6 H, Me, *J*(PH) 7, *J*(PtH) 19], 1.64, 1.77 [d × 2, 6 H, Me, *J*(PH) 11, *J*(PtH) 33], 2.35 (s, br, 1 H, CH of $C_2B_9H_{10}$),[h] 7.17–7.80 (m, 25 H, Ph)	134.6–128.0 (Ph), 44.4, 40.8 ($C_2B_9H_{10}$), 20.9–17.1 (m, Me)
10b	−5.39 [q, 1 H, BHPt, *J*(BH) 79, *J*(PtH) 663], 1.46, 3.46 (s × 2, 2 H, CH of $C_2B_9H_{11}$), 6.58–7.44 (m, 35 H, Ph)	191.1 [d of d, CO, *J*(RhC) 72, *J*(PC) 21], 144.4 [br, C^1 (PhPt), *J*(PtC) 827], 137.7–122.7 (Ph), 46.9, 40.4 ($C_2B_9H_{11}$)
10c[f]	−4.58 [m, br, 1 H, BHPt, *J*(PtH) 557], 0.87 [d, 3 H, MePt, *J*(PH) 8, *J*(PtH) 77], 1.66 (s, br, 1 H, CH of $C_2B_9H_{11}$), 1.94, 1.97 [d × 2, 6 H, MeP, *J*(PH) 12, *J*(PtH) 47], 3.42 (s, br, 1 H, CH of $C_2B_9H_{11}$), 7.35–7.73 (m, 20 H, Ph)	

[a] Chemical shifts δ in ppm, coupling constants in Hz, measurements at ambient temperatures in CD_2Cl_2. [b] Signals due to BH groups appear as broad unresolved resonances in the range δ *ca.* −2 to +3. [c] Hydrogen-1 decoupled, chemical shifts are positive to high frequency of $SiMe_4$ (δ 0.0). [d] Signals for Ph group are doublets, *J*(PC) *ca.* 2–40 Hz. [e] Resonances due to minor isomer asterisked. [f] Complex too unstable to measure ^{13}C-{^1H} NMR spectrum, see text. [g] Resonances for MePt group of two isomers coincident. [h] Other CH resonance is masked by the Me signals.

the ^{195}Pt–^{31}P coupling constants for the last two signals arises from one PEt_3 group being transoid to the B–Pt bond and the other to the Rh–Pt bond, respectively.

Formation of compound **6** involves loss of molecular hydrogen from **4b**, and addition of PhC≡CPh at the platinum centre. This led to the observation that, in the absence of the alkyne, refluxing solutions of **4b** in thf for several days afforded [RhPt(μ-σ:η^5-7,9-$C_2B_9H_{10}$)(CO)(PEt_3)$_2$(PPh_3)]**7a**. Moreover, the latter on treatment with PhC≡CPh in thf slowly forms **6**. Although **7a** slowly forms when thf solutions of **4b** are refluxed, in contrast compound **4a** decomposes on heating for several days in this solvent. Data characterising **7a** are given in Tables 1, 3 and 4. Again the ^{11}B-{^1H} NMR spectrum shows a diagnostic deshielded peak[3] for the B–Pt group [δ 43.8, *J*(PtB) 538 Hz]. The ^{31}P-{^1H} NMR spectrum shows the expected three resonances: a doublet at δ 36.6 [PRh, *J*(RhP) 151], and two singlets at δ 28.4 and 18.6 (PPt), with *J*(PtP) 1908 and 4858 Hz, respectively. The signal at δ 28.4 is very broad, which therefore allows us to assign it to the phosphine group transoid to the B–Pt bond, the *trans* coupling to the quadrupolar ^{11}B causing the extreme broadening.[3] The values of the ^{195}Pt–^{31}P coupling constants are noteworthy, the $^{31}PEt_3$ group transoid to the Rh–Pt bond having a much larger coupling constant (4858 Hz) than that for the ligand cisoid to the metal–metal and transoid to the B–Pt bond (1908 Hz). This is also as one would expect.[3]

In the ^1H NMR spectrum (Table 3) the signals for the ethyl groups appear as broad multiplets, presumably due to their displaying dynamic behaviour.

Formation of compound **7a** from **4b** may proceed through the intermediate **8a**, with a B–H ⟶ Pt exopolyhedral bond. Reductive elimination of molecular hydrogen from **8a**, accompanied by recapture of a PEt_3 ligand, would then yield **7a**. Such a pathway has precedent from previous results. Thus the reaction between [NEt_4][W(≡$CC_6H_3Me_2$-2,6)(CO)$_2$(η^5-7,8-$C_2B_9H_9Me_2$)] and [PtH(Me_2CO)(PEt_3)$_2$][BF_4] initially affords [WPtH(μ-$CC_6H_3Me_2$-2,6)(CO)$_2$(PEt_3)(η^5-7,8-$C_2B_9H_9Me_2$)], a compound containing both a bridging B–H ⟶ Pt and a terminal Pt–H group.[3b] This product, however, readily releases hydrogen to give a mixture of the dicarbonyl complex [WPt(μ-$CC_6H_3Me_2$-2,6)(μ-σ:η^5-$C_2B_9H_8Me_2$)(CO)$_2$(PEt_3)] and the tricarbonyl complex **2**. The latter forms by addition of a CO group to the electronically unsaturated Pt(PEt_3) fragment in the former species. In view of these observations, and the formation of **7a** from **4b**, reactions between the salts **3** and the platinum compounds [PtCl(R)L_2] (R = Me or Ph; L = PEt_3, PPh_3 or PMe_2Ph) were investigated. It was anticipated that these reactions would yield products with B–Pt bonds similar to that in **7a** *via* the loss of CH_4 or C_6H_6 from intermediates akin to **8a**. Moreover, by suitable fine tuning of the tertiary phosphine ligands it was hoped that it might be possible to

Table 4 Boron-11 and phosphorus-31 NMR data[a] for the complexes

Compound	^{11}B[b] (δ)	^{31}P[c] (δ)
4b	−6.2 (1 B), −9.4 (2 B), −11.2 (1 B), −12.8 (1 B), −16.3 (1 B), −20.4 (2 B), −25.4 (1 B)	36.7 [d, PRh, *J*(RhP) 126], 21.1 [d, PPt, *J*(RhP) 13, *J*(PtP) 4131], 4.2 [s, PPt, *J*(PtP) 2699]
6	42.9 [1 B, BPt, *J*(PtB) 659], 1.3 (1 B), −5.9 (1 B), −9.3 (2 B), −16.4 (1 B), −18.8 (1 B), −21.5 (1 B), −26.9 (1 B)	35.8 [d, PRh, *J*(RhP) 149], [d] 26.2 [s, vbr, PPt, *J*(PtP) 1910], 13.5 [s, PPt, *J*(PtP) 4875]
7a	43.8 [1 B, BPt, *J*(PtB) 538], −7.7 (1 B), −10.0 (3 B), −16.2 (1 B), −18.7 (1 B), −20.6 (1 B), −27.8 (1 B)	36.6 [d, PRh, *J*(RhP) 151], [d] 28.4 [s, vbr, PPt, *J*(PtP) 1908], 18.6 [s, br, PPt, *J*(PtP) 4858]
7b	52.3 [1 B, BPt, *J*(PtB) 635], −6.8 to −27.7 (vbr, 8 B)	37.4 [d, br, PRh, *J*(RhP) 140], 25.4 [d of d, PPt, *J*(RhP) 8, *J*(PP) 4, *J*(PtP) 4463]
7c[e]	*46.7, 44.4 [1 B, BPt, *J*(PtB) 586], 1.7 to −27.5 (vbr, 8 B)	36.6 [d, PRh, *J*(RhP) 153], *36.3 [d, PRh, *J*(RhP) 147], [d] 9.1 [s, vbr, PPt, *J*(PtP) 1952], [d] *8.1 [s, vbr, PPt, *J*(PtP) 1945], −10.0 [s, PPt, *J*(PtP) 4921], *−10.1 [s, PPt, *J*(PtP) 4906]
8c	13.9 [1 B, BHPt, *J*(HB) 82, *J*(PtB) 98], −7.7 to −24.4 (vbr, 8 B)	35.1 [d, br, PRh, *J*(RhP) 147], 15.4 [s, PPt, *J*(PtP) 4108]
8d[e]	*23.2 [1 B, BHPt, *J*(HB) 79, *J*(PtB) 122], 17.7 [1 B, BHPt, *J*(HB) 85, *J*(PtB) 122], −0.2 to −24.8 (vbr, 8 B)	37.5 [d, PRh, *J*(RhP) 149], *37.0 [d, PRh, *J*(RhP) 137], *25.4 [s, PPt, *J*(PtP) 3806], 24.6 [s, PPt, *J*(PtP) 4086]
9a	48.3 [1 B, BPt, *J*(PtB) 598], −4.9 (1 B), −9.2 (3 B), −13.4 (1 B), −15.1 (1 B), −19.6 (1 B), −28.1 (1 B)	32.3 [d, br, PRh, *J*(RhP) 124], [d] 29.8 [s, vbr, PPt, *J*(PtP) 2020], 20.9 [s, br, PPt, *J*(PtP) 4376]
9b	49.2 [1 B, BPt, *J*(PtB) 634], −4.6 (1 B), −8.9 (3 B), −13.7 (2 B), −19.7 (1 B), −27.4 (1 B)	33.2 [d, PRh, *J*(RhP) 128], [d] 7.3 [s, vbr, PPt, *J*(PtP) 2088], −9.0 [s, PPt, *J*(PtP) 4740]
10b	27.4 [1 B, BHPt, *J*(HB) 79], −10.3 to −30.2 (vbr, 8 B)	36.7 [d, PRh, *J*(RhP) 149], 16.5 [s, br, PPt, *J*(PtP) 4110]
10c	28.9 [1 B, BHPt, *J*(HB) 67], −8.8 (3 B), −11.8 (1 B), −14.5 (2 B), −19.3 (1 B), −27.8 (1 B)	37.0 [d, PRh, *J*(RhP) 141], −4.2 [s, br, PPt, *J*(PtP) 4028]

[a] Chemical shifts δ in ppm, coupling constants in Hz, measurements in CD_2Cl_2 at ambient temperatures. [b] Hydrogen-1 decoupled, chemical shifts are positive to high frequency of BF_3·Et_2O (external). The ^1H–^{11}B couplings were measured from fully coupled ^{11}B NMR spectra. [c] Hydrogen-1 decoupled, chemical shifts are positive to high frequency of 85% H_3PO_4 (external). [d] Broadness of signal due to phosphine group being transoid to B–Pt bond. [e] Peaks asterisked are due to a minor isomer (see text).

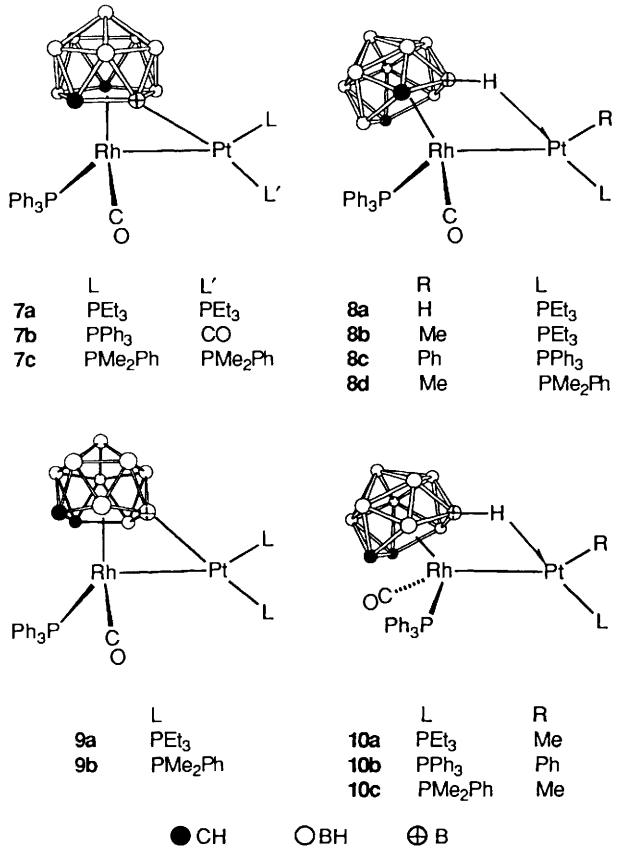

detect or even isolate stable complexes of type **8** (R = Me or Ph), prior to their conversion into species of type **7**.

Treatment of compound **3b** with $[PtCl(Me)(PEt_3)_2]$ in thf, in the presence of $TlBF_4$ to facilitate the removal of the chloride ion as TlCl, afforded **7a**. There was no evidence for an intermediate **8b**, a result which was not unexpected in view of the direct formation of **7a** from solutions of **4b**. A similar reaction between **3a** and $[PtCl(Me)(PEt_3)_2]$ gave $[RhPt(\mu\text{-}\sigma{:}\eta^5\text{-}7,8\text{-}C_2B_9H_{10})(CO)(PEt_3)_2(PPh_3)]$ **9a**. Formation of the latter was accompanied by that of $[Rh_2(PPh_3)_2(\eta^5\text{-}7,8\text{-}C_2B_9H_{11})_2]$, a species observed in several reported reactions of **3a**.[5] There was no evidence for an intermediate complex **10a** in the synthesis of **9a**, just as there was no observable intermediate **8b** in the synthesis of **7a**. Isolation of the dirhodium compound as a side product accounts for the relatively low yield of **9a**. The latter was also prepared by treating $[PtCl(Ph)(PEt_3)_2]$ with **3a**, a process which apparently results in release of benzene, instead of loss of methane when $[PtCl(Me)(PEt_3)_2]$ is employed as the precursor. Data characterising **9a** are given in Tables 1, 3 and 4. In the ^{11}B-{^1H} NMR spectrum (Table 4) the resonance for the BPt group is seen at δ 48.3 [*J*(PtB) 598 Hz], and in the ^{31}P-{^1H} NMR spectrum there are the expected three signals for the non-equivalent ^{31}P nuclei. As for **7a**, one of the PPt signals is extremely broad, with an appreciably smaller ^{195}Pt–^{31}P coupling constant than the other (2020 *versus* 4376 Hz), and may therefore be assigned to the $^{31}PEt_3$ group transoid to the B–Pt bond (see above).

On the basis of earlier work, including the X-ray diffraction results for $[RhPt\{\sigma\text{-}C(C_6H_4Me\text{-}4)\text{=}C(C_6H_4Me\text{-}4)H\}(CO)(PEt_3)(PPh_3)(\eta^5\text{-}7,8\text{-}C_2B_9H_{11})]$, an analogue of **5**,[1b] it is reasonable to assume that it is the boron atom β to the carbons in the co-ordinating 7,8-C_2B_3 face which is the origin of the exopolyhedral B–H ⟶ Pt interaction in the presumed intermediate **10a**. It is suggested that it is the same β-boron atom which is involved in the B–Pt σ bond of **9a**, as indicated in the structural formula shown. However, it is not impossible for one of the borons α to the two carbons to form the exopolyhedral linkage, because in both cases the cage CH vertices would be inequivalent, as is observed in both the ^1H and ^{13}C-{^1H} NMR spectra, due to the asymmetry of the rhodium centre. Nevertheless, attachment of the platinum to the β-boron in **9a** would seem to be the more reasonable assumption. Needless to say an X-ray structure would resolve this matter definitively, but unfortunately it was not possible to obtain suitable crystals.

Reactions between the salts **3** and $[PtCl(Ph)(PPh_3)_2]$ were next investigated. It was thought that if the platinum atom was

ligated by PPh_3, rather than the more strongly donating PEt_3 group, then reductive elimination of benzene might be inhibited and thus allow isolation of the compounds **8c** and **10b**, prior to their decomposition to form species with B–Pt exopolyhedral σ bonds. This premise was supported by the experimental results.

The reagents **3a**, $[PtCl(Ph)(PPh_3)_2]$, and $TlBF_4$ in acetone over a period of several hours at room temperature gave $[RhPtPh(CO)(PPh_3)_2(\eta^5\text{-}7,8\text{-}C_2B_9H_{11})]$ **10b**. The NMR data (Tables 3 and 4) were in complete accord with the proposed structure, and the product was further characterised by microanalysis (Table 1). The ^1H NMR spectrum showed a diagnostic quartet signal for the B–H ⟶ Pt system at δ −5.39 [J(BH) 79 Hz], with ^{195}Pt–^1H satellite peaks [J(PtH) 663 Hz]. In confirmation, the ^{11}B-{^1H} NMR spectrum displayed a resonance at δ 27.4 for one boron nucleus, the other eight borons giving rise to the usual broad overlapping peaks, which were observed in the range δ −10.3 to −30.2. In a fully coupled ^{11}B spectrum the peak at δ 27.4 became a doublet [J(HB) 79 Hz]. The ^1H–^{11}B coupling is of the expected magnitude for a three-centre two-electron B–H ⟶ M bond. Two-centre B–H bonds have J(HB) values of *ca.* 130 Hz.[6]

The ^{31}P-{^1H} NMR spectrum of compound **10b** revealed two resonances. A doublet at δ 36.7 [J(RhP) 149 Hz] may be assigned to the $RhPPh_3$ group, while a broad peak at δ 16.5 is ascribed to the $PtPPh_3$ fragment. The latter signal displays ^{195}Pt–^{31}P satellite peaks [J(PtP) 4110 Hz]. In the ^{31}P-{^1H} NMR spectrum of $[WPtH(\mu\text{-}CC_6H_3Me_2\text{-}2,6)(CO)_2(PEt_3)(\eta^5\text{-}7,8\text{-}C_2B_9H_9Me_2)]$, a molecule mentioned above[3b] also having a B–H ⟶ Pt group like **10b**, but with a $PtH(PEt_3)$ group instead of a $PtPh(PPh_3)$ fragment, the ^{195}Pt–^{31}P coupling (3072 Hz) is somewhat smaller. The tungsten–platinum compound releases H_2 to yield $[WPt(\mu\text{-}CC_6H_3Me_2\text{-}2,6)(\mu\text{-}\sigma\text{:}\eta^5\text{-}7,8\text{-}C_2B_9H_8Me_2)(CO)_2(PEt_3)]$. The latter, with a B–Pt σ bond, exists as two isomers and these show ^{195}Pt–^{31}P coupling of 4300 and 4570 Hz, respectively, in the ^{31}P-{^1H} NMR spectrum, values comparable with that for **10b**. The isomerism in the tungsten–platinum compound is attributed to the existence of species in which the B–Pt linkage involves either a boron atom which is α to the two carbons in the open pentagonal face of the *nido*-C_2B_9 cage ligating the tungsten, or a boron which is β to the carbons. An X-ray diffraction study[3b] on the major isomer (>90%) revealed that it is the β-boron in the CCB*B*B ring which forms the B–Pt bond. We assume that in **10b** it is also the β-boron in the C_2B_3 ring which forms the exopolyhedral bond, as has been established by X-ray diffraction in the structurally related complex $[Rh_2(CO)_2(PPh_3)_2(\eta^5\text{-}7,8\text{-}C_2B_9H_{11})]$ in which the Rh–Rh bond is spanned by a cage B_β–H ⟶ Rh linkage.[1a] However, although for diagrammatic purposes the complex has been represented with the Ph group cisoid and the phosphine group transoid to the B–H ⟶ Pt bond, there is no actual direct NMR evidence for this arrangement. It is possible for them to be arranged the opposite way around relative to the B–H ⟶ Pt bond. For **10b** the value of the ^{195}Pt–^{31}P coupling constant does not provide any evidence one way or the other.

Surprisingly, thf solutions of compound **10b** were stable at ambient temperatures over long periods and even at reflux temperatures did not afford a product with a B–Pt σ bond. Under reflux conditions partial decomposition occurred. In contrast with these results employing **3a** as the reagent, the reaction between **3b** and $[PtCl(Ph)(PPh_3)_2]$, in the presence of $TlBF_4$, yields a mixture of $[RhPtPh(CO)(PPh_3)_2(\eta^5\text{-}7,9\text{-}C_2B_9H_{11})]$ **8c**, $[RhPt(\mu\text{-}\sigma\text{:}\eta^5\text{-}7,9\text{-}C_2B_9H_{10})(CO)_2(PPh_3)_2]$ **7b**, and a minor side-product believed to be $[Rh_2(PPh_3)_2(\eta^5\text{-}7,9\text{-}C_2B_9H_{11})_2]$ (see Experimental section), an analogue of the previously characterised species $[Rh_2(PPh_3)_2(\eta^5\text{-}7,8\text{-}C_2B_9H_{11})_2]$.[5] It was not possible to obtain satisfactory microanalytical data for **8c** because of its ready decomposition into **7b**, a process which involves capture of a CO molecule.

Compound **7b** could be obtained analytically pure by treating mixtures containing **8c** with CO, followed by chromatography on silica, under which conditions the latter complex is completely transformed into the former. Formation of the side-product $[Rh_2(PPh_3)_2(\eta^5\text{-}7,9\text{-}C_2B_9H_{11})_2]$ is not surprising, since formation of **7b** from **8c** requires acquisition of a CO molecule, presumably from the precursor **3b**, and this would release a $Rh(PPh_3)(\eta^5\text{-}7,9\text{-}C_2B_9H_{11})$ fragment which could dimerise to afford the small amounts of the dirhodium compound observed.

The spectroscopic data for compound **8c** fully characterise this species. The IR spectrum displays a single CO band at 1996 cm^{-1}. Although a meaningful ^{13}C-{^1H} NMR spectrum could not be measured, because of the aforementioned ready conversion into **7b**, the ^1H NMR spectrum showed a quartet at δ −5.30 [J(BH) 82, J(PtH) 361 Hz] diagnostic for a B–H ⟶ Pt group. The presence of the latter was unambiguously confirmed by the ^{11}B-{^1H} NMR spectrum which had a resonance at δ 13.9 [J(PtB) 98 Hz] with an intensity corresponding to one boron nucleus. In a fully coupled ^{11}B spectrum this signal became a doublet [J(HB) 82 Hz]. The ^{31}P-{^1H} NMR spectrum revealed two signals of equal intensity in agreement with the formulation proposed, and these were a broad doublet at δ 35.1 [PRh, J(RhP) 147 Hz] and a singlet at δ 15.4 [PtP, J(PtP) 4108 Hz]. Once again the structure has been drawn with the R group cisoid to the B–H ⟶ Pt bond, although, as for **10b**, it might in actuality be transoid. However, the cisoid representation favours the elimination of RH, a process that must take place in the conversion into **7b**. The H and the R groups need, at some point, to have a *cis* relationship to one another, although the precise mechanism for loss of RH is uncertain. One may speculate that release of RH either involves formation of a B–Pt bond, with formal transfer of the H from the B to the Pt to give a terminal Pt–H group, before reductive elimination of RH, or that the elimination occurs simultaneously with the formation of the B–Pt bond. Either pathway is possible, and in agreement with the idea that a B–H ⟶ M interaction is an intermediate on the route to formal oxidative addition of BH to a metal centre.

The data for compound **7b** are also in complete accord with the structural formula depicted. Thus in the IR spectrum there are two CO bands at 2046 and 1993 cm^{-1}. As expected, the ^1H NMR spectrum showed no relatively deshielded resonance characteristic of a B–H ⟶ Pt bridge system. In the ^{11}B-{^1H} NMR spectrum there are broad overlapping resonances in the range δ −6.8 to −27.7, but there is also a single peak corresponding in intensity to one boron nucleus at δ 52.3 [J(PtB) 635 Hz], and this signal is attributable to the BPt group.[3] The ^{31}P-{^1H} NMR spectrum has signals for the PRh and PPt groups at δ 37.4 [J(RhP) 140 Hz] and 25.4 [J(RhP) 8, J(PP) 4, J(PtP) 4463 Hz]. The sharpness of the PPt signal, and the magnitude of the ^{195}Pt–^{31}P coupling, allow us to say with confidence that the phosphine is cisoid to the B–Pt bond and that it is the CO group that is transoid to it. This is supported by the ^{13}C-{^1H} NMR spectrum (Table 3), which displayed a signal due to the CO ligand on the rhodium, but did not show a peak for the PtCO group. This is not surprising if the PtCO group is transoid to a B–Pt bond. Such an arrangement would cause the signal to be extremely broad and, this, together with the anticipated high multiplicity of the resonance, due to coupling with the other various spin-active nuclei, would result in the peaks being hidden by a poor signal-to-noise effect. Moreover, this arrangement of the $Pt(CO)(PPh_3)$ group, with the CO transoid and the phosphine preferentially cisoid to the B–Pt bond, is in agreement with the structures of the complexes $[WPt(\mu\text{-}CC_6H_3Me_2\text{-}2,6)(\mu\text{-}\sigma\text{:}\eta^5\text{-}7,8\text{-}C_2B_9H_8Me_2)(CO)_2(PEt_3)]$ and **2**,[3b] mentioned above.

Isolation of the compounds **8c** and **10b** in which the platinum carries a PPh_3 ligand, and the failure to identify related species with PEt_3 groups, prior to their conversion into the more stable products with B–Pt bonds, prompted studies on reactions between $[PtCl(Me)(PMe_2Ph)_2]$ and the salts **3**. The donor ability of PMe_2Ph lies between that of PEt_3 and PPh_3 and it

was of interest to establish whether, by using the reagent $[PtCl(Me)(PMe_2Ph)_2]$, intermediates with B–H ⟶ Pt bonds would be observed prior to their affording products with the thermodynamically more stable B–Pt linkages.

The reaction between compounds **3a** and $[PtCl(Me)(PMe_2Ph)_2]$ in thf gave after *ca.* 4 h at room temperature the labile complex $[RhPtMe(CO)(PMe_2Ph)(PPh_3)(\eta^5\text{-}7,8\text{-}C_2B_9H_{11})]$ **10c**, data for which are given in Tables 1, 3 and 4. The compound shows one CO absorption (1996 cm^{-1}) in its IR spectrum, and was observed to be unstable in solution, affording $[RhPt(\mu\text{-}\sigma\text{:}\eta^5\text{-}7,8\text{-}C_2B_9H_{10})(CO)(PMe_2Ph)_2(PPh_3)]$ **9b** within a few hours. Hence satisfactory microanalytical data could not be obtained for **10c**, nor could its $^{13}C\text{-}\{^1H\}$ NMR spectrum be recorded, the resonances seen over the period of the measurement being those of **9b**. Indeed, if the reaction between **3a** and $[PtCl(Me)(PMe_2Ph)_2]$ is allowed to proceed for several hours compound **9b** is the only product isolated.

Nevertheless, compound **10c**, was identified by its ^1H, $^{11}B\text{-}\{^1H\}$, and $^{31}P\text{-}\{^1H\}$ NMR spectra, recorded on samples recovered in the initial stages of the overall reaction. Thus a broad resonance at δ −4.58 in the ^1H NMR spectrum, with $^{195}Pt\text{–}^1H$ satellite peaks [J(PtH) 557 Hz], is assigned to the B–H ⟶ Pt group, and the presence of this moiety was confirmed from the $^{11}B\text{-}\{^1H\}$ spectrum with a signal at δ 28.9. The latter became a doublet [J(HB) 67 Hz] in an $^{11}B\text{–}^1H$ spectrum. The ^1H NMR spectrum also showed a doublet resonance due to the PtMe group at δ 0.87 [J(PH) 8, J(PtH) 77 Hz], as well as all the other expected peaks. The $^{31}P\text{-}\{^1H\}$ NMR spectrum displayed two resonances, of equal intensity, for the PRh [δ 37.0, J(RhP) 141 Hz] and PPt [δ −4.2, J(PtP) 4028 Hz] groups. Although, once again, it is impossible to assign the configuration of the PtR(L) moiety unambiguously with respect to the rest of the molecule.

Compound **9b** was fully characterised by the data given in Tables 1, 3 and 4. In the $^{11}B\text{-}\{^1H\}$ NMR spectrum the resonance for the BPt group is seen at δ 49.2 [J(PtB) 634 Hz], and, as for **9a**, we propose that it is the β-boron which is involved in forming the B–Pt σ bond. The $^{31}P\text{-}\{^1H\}$ NMR spectrum had signals for the three non-equivalent phosphorus nuclei at δ 33.2 (RhP), 7.3 and −9.0 (PPt), with the usual $^{103}Rh\text{–}$ and $^{195}Pt\text{–}^{31}P$ couplings (Table 4). Since the signal at δ 7.3 is extremely broad it is assigned to the phosphine group transoid to the B–Pt bond. The $^{13}C\text{-}\{^1H\}$ NMR spectrum (Table 3) was weak, due to poor solubility of the complex, and thus the CO resonance, which would be split by ^{103}Rh and ^{31}P coupling, was not seen. However, the IR spectrum established the presence of the CO ligand with a band at 1980 cm^{-1}. Characteristic peaks for the cage CH vertices were observed in the $^{13}C\text{-}\{^1H\}$ NMR spectrum of **9b** at δ 40.8 and 44.4.

The reaction between compound **3b** and $[PtCl(Me)(PMe_2Ph)_2]$ was also investigated, yielding $[RhPt(\mu\text{-}\sigma\text{:}\eta^5\text{-}7,9\text{-}C_2B_9H_{10})(CO)(PMe_2Ph)_2(PPh_3)]$ **7c** *via* the initially formed $[RhPtMe(CO)(PMe_2Ph)(PPh_3)(\eta^5\text{-}7,9\text{-}C_2B_9H_{11})]$ **8d**. The latter was very labile, readily affording **7c**. Hence microanalytical and $^{13}C\text{-}\{^1H\}$ NMR data were not obtained. Both **7c** and **8d** were each produced as a mixture of two isomers, as deduced from a duplication of peaks in the NMR spectra. These isomers were formed in *ca.* 2:1 ratio, as estimated from relative peak intensities in the spectra. The isomerism is believed to be due to the two possible orientations for the exopolyhedral B–H ⟶ Pt and B–Pt bonds with respect to the $Rh(CO)(PPh_3)$ fragments. For each complex in one configuration these linkages would lie on the same side of the Rh–Pt bond as the Rh–CO vector, and in the other on the same side as the Rh–P vector.

The ^1H NMR spectrum of compound **8d** (Table 3) showed a quartet signal for the major isomer at δ −4.07 [J(BH) 85 Hz] attributable to the B–H ⟶ Pt moiety, and correspondingly in the $^{11}B\text{-}\{^1H\}$ NMR spectrum there was a resonance at δ 17.7 [J(PtB) 122 Hz] which in an $^{11}B\text{–}^1H$ spectrum became a doublet [J(HB) 85 Hz]. The presence of the MePt group in **8d** was revealed in the ^1H NMR spectrum by a doublet resonance at δ 0.49 [J(PH) 4 Hz] corresponding in intensity to three protons, and this signal had ^{195}Pt satellite peaks [J(PtH) 86 Hz]. The $^{31}P\text{-}\{^1H\}$ NMR spectrum (Table 4) displayed the expected two resonances for the PRh and PPt groups in each isomer. Again, as for **8c**, **10b** and **10c**, the molecule is displayed with the R group cisoid to the B–H ⟶ Pt bond, the most likely configuration at the platinum centre.

The NMR data for compound **7c** were in agreement with its formulation. In the $^{11}B\text{-}\{^1H\}$ NMR spectrum resonances at δ 46.7 and 44.4 are attributable to the BPt groups of the minor and major isomer, respectively. Similarly, each isomer shows in its $^{31}P\text{-}\{^1H\}$ NMR spectrum a doublet resonance for the PRh group and two signals for the non-equivalent PMe_2Ph ligands, which we were once again able to assign to the cisoid and transoid (relative to the B–Pt bond) phosphine. The resonances observed in the ^1H and $^{13}C\text{-}\{^1H\}$ NMR spectra (Table 3) were also in accord with the structural formula shown.

Several conclusions can be drawn from the results described in this paper. It is evident that the complexes with B–Pt exopolyhedral bonds are formed from intermediates with B–H ⟶ Pt linkages. We have commented above that formation of **7b** from **8c** requires capture of a CO molecule. A similar capture of a tertiary phosphine ligand is necessary in the formation of **7c**, **9a** and **9b**, from **8d**, **10a** and **10c**, respectively. The phosphine molecule required for this step would be present in the mixture as a result of it having been displaced from the platinum in the reagents $[PtCl(R)L_2]$ upon initial formation of **8d**, **10a** or **10c**. Moreover, it was observed that if **8d** and **10c** are isolated, then subsequent conversion into **7c** and **9b**, respectively, may be promoted by the addition of 1 equivalent of PMe_2Ph. In the case of **8c**, however, capture of CO is favoured to give **7b**, rather than addition of PPh_3 at the platinum centre. Reductive elimination of RH molecules from the species with B–H ⟶ Pt bonds is favoured by increasing the nucleophilicity at the platinum centre. Thus the syntheses of the compounds **7** and **9** from **8** and **10**, respectively, are more facile in the order $L = PEt_3 > PMe_2Ph > PPh_3$. There is evidence also that complexes with $Rh(\eta^5\text{-}7,9\text{-}C_2B_9H_{11})$ groups afford species with B–Pt bonds more readily than those with $Rh(\eta^5\text{-}7,8\text{-}C_2B_9H_{11})$. Thus **4b** yields **7a** whereas, under similar conditions, **4a** does not give **9a**. Similarly, **10b** is very stable, whereas **8c** affords **7b**. It is interesting to speculate that this behaviour may be related to the distortions in the η^5-BCBCB pentagonal ring in the complexes of type **8**, which perhaps move the H atom in the B–H ⟶ Pt bridge closer to the platinum, thereby weakening the B–H linkage and thus promoting the loss of RH. Finally, in some of the reactions of the salts **3** with the compounds $[PtCl(R)L_2]$ it was observed, by IR spectroscopy, that a very labile intermediate [ν_{max}(CO) *ca.* 1963–1970 cm^{-1}] was the initial species formed. The latter decomposed very rapidly to give the observed products. Although the lability of these initial intermediates precluded any attempt to use NMR spectroscopy to obtain structural information, we may speculate that they are the σ-bonded complexes,$[(\eta^5\text{-}7,n\text{-}C_2B_9H_{11})(Ph_3P)(OC)Rh\text{–}PtR(L)_2]$ (n = 8 or 9). Indeed, it is proposed that these species are always formed initially, but are not always detected.

Experimental

Light petroleum refers to that fraction of b.p. 40–60 °C, and all solvents were freshly distilled over appropriate drying agents prior to use. Chromatography columns *ca.* 15 cm long and 3 cm in diameter were packed with alumina (Brockmann activity II) or silica (70–230 mesh). Celite pads, used to remove TlCl by filtration, were *ca.* 3 cm thick. All experiments were carried out under nitrogen using Schlenk-tube techniques. The NMR measurements were made using a Bruker AMX 360 MHz spectrometer and IR spectra were recorded with a Bruker IFS 25 instrument. The reagents $[NEt_4][Rh(CO)(PPh_3)(\eta^5\text{-}7,n\text{-}C_2B_9H_{11})]$ (n = 8 or 9)[4] and $[PtCl(R)L_2]$[7] were prepared by procedures described earlier.

Synthesis and Reactions of $[RhPt(\mu\text{-}H)(\mu\text{-}CO)(PEt_3)_2(PPh_3)(\eta^5\text{-}7,9\text{-}C_2B_9H_{11})]$.—(*i*) A mixture of compound **3b** (0.20 g, 0.31 mmol), $[PtCl(H)(PEt_3)_2]$ (0.14 g, 0.31 mmol), and $TlBF_4$ (0.098 g, 0.34 mmol) in thf (25 cm^3) was stirred at room temperature for 4 h, after which time an IR spectrum showed that the reaction was complete. The orange-brown suspension was filtered through Celite, following which solvent was removed *in vacuo*. The residue was dissolved in CH_2Cl_2–light petroleum (10 cm^3, 3:2) and chromatographed on alumina at −10 °C. Elution with the same solvent mixture removed initially a trace of a pink-orange fraction, followed by an orange eluate. Solvent was removed *in vacuo* from the latter, and the residue was crystallised from CH_2Cl_2–light petroleum (*ca.* 30 cm^3, 1:5) to give orange *microcrystals* of $[RhPt(\mu\text{-}H)(\mu\text{-}CO)(PEt_3)_2(PPh_3)(\eta^5\text{-}7,9\text{-}C_2B_9H_{11})]$ **4b** (0.24 g), washed with light petroleum (2 × 10 cm^3) and dried *in vacuo*.

(*ii*) Compound **4b** (0.15 g, 0.16 mmol) was refluxed in thf (25 cm^3) for 5 d, during which time the colour slowly changed from orange to brown, and an IR measurement showed that all the starting complex had been consumed. Solvent was removed *in vacuo*, the brown residue was dissolved in CH_2Cl_2 (10 cm^3), and the solution was adsorbed on silica (*ca.* 2 g) by removal of solvent *in vacuo*. The dry powder was transferred to the top of a silica chromatography column, cooled to −10 °C. Elution with CH_2Cl_2–light petroleum (1:4) removed a trace of unidentified material. Continued elution with CH_2Cl_2–light petroleum (2:3) removed a yellow fraction shown to contain the product. Increasing the proportion of CH_2Cl_2 further (3:2) removed a small amount of **4b**, identified by IR spectroscopy. Removal of solvent *in vacuo* from the yellow eluate and crystallisation of the residue from CH_2Cl_2–light petroleum (*ca.* 15 cm^3, 1:6) gave yellow *microcrystals* of $[RhPt(\mu\text{-}\sigma\text{:}\eta^5\text{-}7,9\text{-}C_2B_9H_{10})(CO)(PEt_3)_2(PPh_3)]$ **7a** (0.14 g), after washing with light petroleum (2 × 5 cm^3) and drying *in vacuo*.

(*iii*) A mixture of compound **7a** (0.15 g, 0.16 mmol) and PhC≡CPh (0.043 g, 0.24 mmol) in thf (15 cm^3) was stirred for 3 d, after which time solvent was removed *in vacuo*. The residue was dissolved in CH_2Cl_2 (*ca.* 10 cm^3) and adsorbed on silica. The powder obtained was transferred to the top of a silica-packed chromatography column held at −10 °C. Elution with CH_2Cl_2–light petroleum (1:4) removed a trace of an unidentified pink eluate. Continued elution with CH_2Cl_2–light petroleum (3:7) removed the major fraction which was yellow. Removal of solvent *in vacuo*, followed by crystallisation of the residue from CH_2Cl_2–light petroleum (20 cm^3, 1:15) gave *microcrystals* of $[RhPt(\mu\text{-}\sigma\text{:}\eta^5\text{-}7,9\text{-}C_2B_9H_{10})(CO)(PEt_3)_2(PPh_3)(\eta\text{-}PhC{\equiv}CPh)]$ **6** (0.17 g), washed with light petroleum (2 × 5 cm^3) and dried *in vacuo*.

Complex **6** was also obtained by refluxing **4b** with PhC≡CPh in thf (25 cm^3) for 5 d, the product being isolated as above in lower yield (*ca.* 50%).

Reactions of $[NEt_4][Rh(CO)(PPh_3)(\eta^5\text{-}7,9\text{-}C_2B_9H_{11})]$.—(*i*) A mixture of the compounds **3b** (0.15 g, 0.23 mmol), $[PtCl(Ph)(PPh_3)_2]$ (0.19 g, 0.23 mmol), and $TlBF_4$ (0.073 g, 0.25 mmol) was stirred in thf (25 cm^3). Infrared spectroscopy revealed a transient intermediate [ν_{max}(CO) 1964 cm^{-1}] too labile to be identified. After stirring for *ca.* 2 d an air-sensitive dark orange-brown solution and a grey precipitate of TlCl had formed. Solvent was removed *in vacuo*, the residue extracted with CH_2Cl_2 (2 × 30 cm^3), and the extracts filtered through Celite. Solvent was removed *in vacuo*, and the residue pre-adsorbed on to silica as described above and chromatographed on a silica column, cooled to −10 °C. Elution with CH_2Cl_2–light petroleum (1:4) developed a golden-yellow band which was removed by increasing the polarity of the solvent mixture using CH_2Cl_2–light petroleum (2:3). Trace amounts of mixtures of unidentified minor products were eluted by further increasing the concentration of CH_2Cl_2.

Solvent was removed *in vacuo* from the major golden-yellow eluate. NMR studies revealed that the residue consisted of a mixture of $[RhPtPh(CO)(PPh_3)_2(\eta^5\text{-}7,9\text{-}C_2B_9H_{11})]$ **8c**, $[RhPt(\mu\text{-}\sigma\text{:}\eta^5\text{-}7,9\text{-}C_2B_9H_{10})(CO)_2(PPh_3)_2]$ **7b**, and a product believed to be $[Rh_2(PPh_3)_2(\eta^5\text{-}7,9\text{-}C_2B_9H_{11})_2]$, formed in *ca.* 10:2:1 ratio, based on the relative intensities of the ^{31}P resonances. Compound **8c** was identified from its ^1H, $^{31}P\text{-}\{^1H\}$, and $^{11}B\text{-}\{^1H\}$ NMR spectra (Tables 3 and 4), and by comparison of these data with those for **10b**. It was observed that, if a solution of the mixture was allowed to stand, compound **8c** converted into **7b**. Rechromatography of the mixture, as described above, then allowed separation of microanalytically pure *microcrystals* of the latter complex (0.035 g, 15%), after washing with light petroleum (2 × 10 cm^3) and drying *in vacuo*. However, **7b** can be obtained in much better yield (0.10 g, 45%), using the same quantities of reagents, by allowing the mixture to stir for 24 h and then bubbling CO through it for *ca.* 30 min. Using this procedure, compound **8c** was not among the products, and **7b** could be separated from $[Rh_2(PPh_3)_2(\eta^5\text{-}7,9\text{-}C_2B_9H_{11})_2]$. Identification of the small amounts of the latter formed (*ca.* 20 mg) was based on comparison of the NMR data (^1H, $^{31}P\text{-}\{^1H\}$, $^{11}B\text{-}\{^1H\}$ and ^{11}B–^1H) with those of the known isomeric species $[Rh_2(PPh_3)_2(\eta^5\text{-}7,8\text{-}C_2B_9H_{11})_2]$.[5]

(*ii*) A mixture of compound **3b** (0.25 g, 0.38 mmol), $[PtCl(Me)(PMe_2Ph)_2]$ (0.20 g, 0.38 mmol), and $TlBF_4$ (0.13 g, 0.46 mmol) was stirred in thf (25 cm^3) for *ca.* 3 d. Solvent was removed *in vacuo*, the residue extracted with CH_2Cl_2 (2 × 30 cm^3), and the extracts filtered through Celite. Solvent was removed *in vacuo* from the dark orange solution obtained, and the residue was pre-adsorbed on silica, as described above. The powder obtained was transferred to the top of a chromatography column of the same material, cooled to −10 °C. Elution with CH_2Cl_2–light petroleum (1:4) removed a trace of an unidentified pink fraction. Further elution with CH_2Cl_2–light petroleum (2:3) gave an orange fraction, from which solvent was removed *in vacuo*. Crystallisation of the residue from CH_2Cl_2–light petroleum (30 cm^3, 1:20) gave mustard-yellow *microcrystals* of $[RhPt(\mu\text{-}\sigma\text{:}\eta^5\text{-}7,9\text{-}C_2B_9H_{10})(CO)(PMe_2Ph)_2(PPh_3)]$ **7c** (0.28 g), after washing with light petroleum (2 × 5 cm^3) and drying *in vacuo*.

The reaction was observed to proceed *via* two intermediates. The first was transient [ν_{max}(CO) at 1963 cm^{-1}] and the second more persistent [ν_{max}(CO) at 1990 cm^{-1}]. If the reaction was stopped after *ca.* 5 h and the mixture worked up as described above, elution of the chromatography column with CH_2Cl_2–light petroleum (3:7) yielded a yellow fraction [ν_{max}(CO) at 1990 cm^{-1}]. The NMR data (Tables 3 and 4) showed that it was $[RhPtMe(CO)(PMe_2Ph)(PPh_3)(\eta^5\text{-}7,9\text{-}C_2B_9H_{11})]$ **8d**. Since

Table 5 Data for crystal structure analysis of compound **4b**

Molecular formula	$C_{33}H_{57}B_9OP_3PtRh\cdot0.5CH_2Cl_2$
M	1000.4
Crystal system	Monoclinic
Space group	$P2_1/n$ (no. 14)
a/Å	11.024(1)
b/Å	23.314(2)
c/Å	16.670(1)
β/°	93.856(7)
U/Å^3	4274.7(6)
Z	4
D_c/Mg m^{-3}	1.55
D_m/Mg m^{-3}	1.54(1)
F(000)	1988
μ(Mo-Kα)/cm^{-1}	38.90
T/K	292
Scan range, ω/°	1.20 + 0.34 tan θ
Radiation	Mo-Kα (λ̄ = 0.710 73 Å)
Data-to-parameter ratio	7.7:1
R, R' (R_{all})	0.0295, 0.0351 (0.045)
S	1.78
Residual density (maximum, minimum/e Å^{-3})	0.87, −1.04

Table 6 Atomic positional parameters (fractional coordinates, $\times 10^4$) for compound **4b** with estimated standard deviations in parentheses

Atom	*x*	*y*	*z*	Atom	*x*	*y*	*z*
Pt	1710(1)	1037(1)	3084(1)	C(64)	127(10)	158(5)	1324(7)
Rh	989(1)	2082(1)	3646(1)	C(65)	3572(8)	947(4)	1462(6)
C(1a)	1253(6)	1324(3)	4162(4)	C(66)	4242(9)	1508(5)	1745(7)
O(1a)	1182(5)	1164(2)	4836(3)	P(3)	−1102(2)	1981(1)	3523(1)
C(1)	1288(7)	3021(3)	3182(4)	C(11)	−1890(6)	2012(3)	4460(4)
C(2)	1796(6)	2605(3)	4731(4)	C(12)	−3160(7)	1993(3)	4442(5)
B(3)	698(9)	2958(4)	4115(5)	C(13)	−3715(8)	1998(4)	5166(5)
B(4)	2857(8)	2316(4)	4171(5)	C(14)	−3030(8)	2017(4)	5884(5)
B(5)	2507(8)	2588(4)	3147(5)	C(15)	−1814(8)	2035(4)	5903(4)
B(6)	3659(8)	2926(4)	3814(6)	C(16)	−1227(7)	2032(3)	5182(4)
B(7)	2662(10)	3366(4)	3200(6)	C(21)	−1780(6)	2549(4)	2867(4)
B(8)	1498(9)	3598(4)	3785(6)	C(22)	−2622(8)	2937(4)	3112(5)
B(9)	1809(9)	3347(4)	4773(6)	C(23)	−3043(9)	3372(5)	2590(6)
B(10)	3164(8)	2948(4)	4792(6)	C(24)	−2643(9)	3418(4)	1841(5)
B(11)	3032(9)	3554(5)	4206(6)	C(25)	−1817(8)	3030(4)	1593(5)
P(1)	2631(2)	243(1)	3645(1)	C(26)	−1361(7)	2618(4)	2109(5)
C(51)	3477(8)	−231(4)	3009(5)	C(31)	−1755(6)	1302(4)	3111(5)
C(52)	4310(9)	−678(4)	3412(6)	C(32)	−2303(8)	1250(4)	2340(5)
C(53)	3738(8)	465(4)	4442(5)	C(33)	−2750(10)	741(4)	2081(6)
C(54)	4775(9)	793(4)	4128(7)	C(34)	−2706(8)	271(4)	2567(6)
C(55)	1629(8)	−231(4)	4185(6)	C(35)	−2161(9)	313(4)	3317(6)
C(56)	666(9)	−531(5)	3633(7)	C(36)	−1668(8)	824(4)	3592(5)
P(2)	1995(2)	919(1)	1719(1)	C(90)*	4725(11)	−130(7)	616(6)
C(61)	1227(7)	1459(4)	1088(4)	Cl(1)*	4216(8)	33(4)	−393(6)
C(62)	1440(9)	1446(4)	197(5)	Cl(2)*	6224(9)	−426(4)	636(5)
C(63)	1465(9)	243(4)	1276(5)				

* Solvent molecule, C(90), Cl(1), and Cl(2) refined at half occupancy.

the latter afforded **7c** so readily it was not possible to obtain meaningful ^{13}C-{^1H} NMR data, nor a microanalysis.

Reactions of [NEt_4][Rh(CO)(PPh_3)(η^5-7,8-$C_2B_9H_{11}$)].—(*i*) The reagents **3a** (0.15 g, 0.23 mmol), [PtCl(Me)(PEt_3)$_2$] (0.11 g, 0.23 mmol), and $TlBF_4$ (0.080 g, 0.27 mmol) were stirred together in thf (20 cm^3) for 45 min. Solvent was removed *in vacuo* and the residue was extracted with CH_2Cl_2 (2 × 30 cm^3), following which the extracts were filtered through Celite to remove TlCl. Solvent was removed *in vacuo*, and the residue was pre-adsorbed on silica, as described above. The powder was transferred to the top of a silica chromatography column maintained at −10 °C. Elution with CH_2Cl_2–light petroleum (2:3) removed traces of uncharacterised material. Continued elution with a 1:1 solvent mixture removed a maroon fraction, identified as [$Rh_2(PPh_3)_2(\eta^5$-7,8-$C_2B_9H_{11})_2$][5] (0.050 g), followed by a greenish yellow band. The eluate from the latter was collected, solvent was removed *in vacuo*, and the residue crystallised from CH_2Cl_2–light petroleum (15 cm^3, 1:10) to afford yellow-green *microcrystals* of [RhPt(μ-σ:η^5-7,8-$C_2B_9H_{10}$)(CO)(PEt_3)$_2$(PPh_3)] **9a** (0.077 g), washed with light petroleum (2 × 5 cm^3) and dried *in vacuo*.

(*ii*) An acetone (25 cm^3) solution of compound **3a** (0.15 g, 0.23 mmol), [PtCl(Ph)(PPh_3)$_2$] (0.19 g, 0.23 mmol), and $TlBF_4$ (0.080 g, 0.27 mmol) was stirred for 12 h. Infrared spectroscopy again revealed a transient intermediate [ν_{max}(CO) 1970 cm^{-1}] too labile to be identified. Solvent was removed *in vacuo*, and the residue extracted with CH_2Cl_2 (2 × 30 cm^3). The extracts were filtered through Celite, solvent was removed *in vacuo*, and the residue dissolved in CH_2Cl_2–light petroleum (*ca.* 5 cm^3, 1:1) and chromatographed on alumina at −10 °C. Elution with the same solvent mixture yielded a green-yellow fraction. Removal of solvent *in vacuo*, followed by crystallisation from CH_2Cl_2–light petroleum (*ca.* 15 cm^3, 1:5), gave yellow-green *microcrystals* of [RhPtPh(CO)(PPh_3)$_2$(η^5-7,8-$C_2B_9H_{11}$)] **10b** (0.15 g), washed with light petroleum (2 × 10 cm^3) and dried *in vacuo*.

(*iii*) A mixture of the compounds **3a** (0.25 g, 0.38 mmol), [PtCl(Me)(PMe_2Ph)$_2$] (0.20 g, 0.38 mmol), and $TlBF_4$ (0.13 g, 0.46 mmol) in thf (25 cm^3) was stirred for *ca.* 4 h. After filtration through Celite, solvent was removed *in vacuo* and the residue adsorbed on silica as described above. The resulting powder was added to the top of a silica-packed chromatography column held at −10 °C. Elution with CH_2Cl_2–light petroleum (1:4) removed two unidentified products formed in trace amounts. Further elution with CH_2Cl_2–light petroleum (2:3) gave a yellow-green solution. Removal of solvent *in vacuo*, and crystallisation of the residue from CH_2Cl_2–light petroleum (25 cm^3, 1:20), afforded yellow *microcrystals* of [RhPtMe(CO)(PMe_2Ph)(PPh_3)(η^5-7,8-$C_2B_9H_{11}$)] **10c** (0.13 g).

Further elution of the column with CH_2Cl_2–light petroleum (1:1) gave a green eluate. Removal of solvent *in vacuo* and crystallisation from the same solvents (20 cm^3, 1:8) afforded green *microcrystals* of [RhPt(μ-σ:η^5-7,8-$C_2B_9H_{10}$)(CO)(PMe_2Ph)$_2$(PPh_3)] **9b** (0.076 g). This product was subsequently isolated in higher yield (*ca.* 37%) by allowing the reaction to proceed for *ca.* 3d before work-up.

Crystal Structure Determination of Compound **4b**.—Crystals of compound **4b** were grown by slow diffusion of a dichloromethane solution into layered light petroleum. The orange rectangular-shaped single crystal (0.26 × 0.28 × 0.94 mm) used in the structural analysis was selected on the basis of optical homogeneity and mounted on an Enraf-Nonius CAD4-F automated diffractometer, equipped with a dense graphite monochromator. Data were collected in the ω–2θ mode at a varied scan rate (0.46 to 3.44° min^{-1}) and in the 2θ range 3.0–40.0° (*h* 0–10, *k* 0–22, *l* −15 to 15). Final unit-cell dimensions and standard deviations were obtained by least-squares fit of 25 well centred high-angle reflections (28 < 2θ < 40°). No significant variations were observed in the intensities of the monitored check reflections (every 2 h, < 1.0%). Thus, crystal stability was verified. All intensity data were corrected for Lorentz and polarisation effects after which an empirical absorption correction, based on high-angle ψ scans,[8] was made (transmission factors: minimum, 0.9578; maximum 0.9998). Of the 4389 measured intensities, 3970 were independent. After averaging the data (R_{int} = 0.0266), 3557

reflections fitted $F_i > 6.0\sigma(F_i)$. Space-group determination was based on systematic absences ($0k0$, $k = 2n + 1$ and $h0l$, $h + l = 2n + 1$). Crystal data, experimental and statistical summaries, and refinement parameters are listed in Table 5.

The structure solution was obtained by employing Patterson and standard difference-map techniques on a personal computer using the SHELXTL-PC[9] package of programs. All non-hydrogen atoms were refined anisotropically using the block full-matrix least-squares procedure. Hydrogen atomic positions were idealised (C–H 0.96, B–H 1.10, Pt–H 1.75 Å) and allowed to ride on their respective bonding atoms with fixed isotropic thermal parameters ($10^3 U_{iso}$ = 80, 60, 50 Å^2). The final cycle of refinement included a secondary extinction correction [g = 2.7(3) × 10^{-4} e^{-2}] and yielded residual indices of $R = [\Sigma(|F_o| - |F_c|)/\Sigma|F_o|] = 0.0295$ and $R' = [\Sigma w(|F_o| - |F_c|)^2/\Sigma w|F_o|^2]^{\frac{1}{2}} = 0.0351$. The quantity minimised was $\Sigma w||F_o| - |F_c||^2$ and the weighting scheme was $w^{-1} = \sigma^2(F) + 0.0004F^2$. The final Fourier difference map was featureless except for a maximum of +0.87 e Å^{-3} in the vicinity of the platinum atom which is quite normal for heavy atoms. Atomic scattering factors were taken from ref. 10. Final non-hydrogen atomic coordinates according to the numbering scheme found in Fig. 1 are presented in Table 6.

Additional material available from the Cambridge Crystallographic Data Centre comprises H-atom coordinates, thermal parameters and remaining bond lengths and angles.

Acknowledgements

We thank the Robert A. Welch Foundation for support under Grants AA-1201 and 0668, and the UK Science and Engineering Research Council for the award of a Research Studentship (to J. E. G.).

References

1 (*a*) J. R. Fernandez, G. F. Helm, J. A. K. Howard, M. U. Pilotti and F. G. A. Stone, *J. Chem. Soc., Dalton Trans.*, 1990, 1747; (*b*) J. E. Goldberg, J. A. K. Howard, H. Müller, M. U. Pilotti and F. G. A. Stone, *J. Chem. Soc., Dalton Trans.*, 1990, 3055; (*c*) M. U. Pilotti, F. G. A Stone and I. Topaloğlu, *J. Chem. Soc., Dalton Trans.*, 1991, 1621; (*d*) M. U. Pilotti, F. G. A. Stone and I. Topaloğlu, *J. Chem. Soc., Dalton Trans.*, 1991, 1355; (*e*) N. Carr, M. C. Gimeno, J. E. Goldberg, M. U. Pilotti, F. G. A. Stone and I. Topaloğlu, *J. Chem. Soc., Dalton Trans.*, 1990, 2253.

2 D. A. Roberts and G. L. Geoffroy, in *Comprehensive Organometallic Chemistry*, eds. G. Wilkinson, F. G. A. Stone and E. W. Abel, Pergamon, Oxford, 1982, vol. 6, sect. 40; R. B. King, P. M. Treichel and F. G. A. Stone, *Chem. Ind. (London)*, 1961, 747.

3 (*a*) M. J. Attfield, J. A. K. Howard, A. N. de M. Jelfs, C. M. Nunn and F. G. A. Stone, *J. Chem. Soc., Dalton Trans.*, 1987, 2219; (*b*) D. D. Devore, J. A. K. Howard, J. C. Jeffery, M. U. Pilotti and F. G. A. Stone, *J. Chem. Soc., Dalton Trans.*, 1989, 303.

4 J. A. Walker, C. B. Knobler and M. F. Hawthorne, *Inorg. Chem.*, 1985, **24**, 2688.

5 R. T. Baker, R. E. King, C. B. Knobler, C. A. O'Con and M. F. Hawthorne, *J. Am. Chem. Soc.*, 1978, **100**, 8266; P. E. Behnken, T. B. Marder, R. T. Baker, C. B. Knobler, M. R. Thompson and M. F. Hawthorne, *J. Am. Chem. Soc.*, 1985, **107**, 932.

6 M. Green, J. A. K. Howard, A. P. James, A. N. de M. Jelfs, C. M. Nunn and F. G. A. Stone, *J. Chem. Soc., Dalton Trans.*, 1987, 81.

7 D. Afzal, P. G. Lenhert and C. M. Lukehart, *J. Am. Chem. Soc.*, 1984, **106**, 3050; H. C. Clark, P. L. Fiess and C. S. Wong, *Can. J. Chem.*, 1977, **55**, 177; J. Chatt and B. L. Shaw, *J. Chem. Soc.*, 1959, 4020; N. Carr, M. C. Gimeno and F. G. A. Stone, *J. Chem. Soc., Dalton Trans.*, 1990, 2617.

8 Vax Structure Determination Package, Enraf-Nonius, Delft, 1982.

9 SHELXTL-PC, Siemens Analytical X-Ray Instruments, Madison, WI, 1989.

10 *International Tables for X-Ray Crystallography*, Kynoch Press, Birmingham, 1974, vol. 4.

Received 6th May 1992; *Paper* 2/02329F